A Closed-Form Nonlinear Model for the Constraint Characteristics of Symmetric Spatial Beams

Shiladitya Sen

Shorya Awtar[1]
e-mail: awtar@umich.edu

Precision Systems Design Lab,
Mechanical Engineering,
University of Michigan,
2350 Hayward Street,
Ann Arbor, MI 48109

The constraint-based design of flexure mechanisms requires a qualitative and quantitative understanding of the constraint characteristics of flexure elements that serve as constraints. This paper presents the constraint characterization of a uniform and symmetric cross-section, slender, spatial beam—a basic flexure element commonly used in three-dimensional flexure mechanisms. The constraint characteristics of interest, namely stiffness and error motions, are determined from the nonlinear load–displacement relations at the beam end. Appropriate assumptions are made while formulating the strain and strain energy expressions for the spatial beam to retain relevant geometric nonlinearities. Using the principle of virtual work, nonlinear beam governing equations are derived and subsequently solved for general end loads. The resulting nonlinear load–displacement relations capture the constraint characteristics of the spatial beam in a compact, closed-form, and parametric manner. This constraint model is shown to be accurate using nonlinear finite element analysis, within a load and displacement range of practical interest. The utility of this model lies in the physical and analytical insight that it offers into the constraint behavior of a spatial beam flexure, its use in design and optimization of 3D flexure mechanism geometries, and its elucidation of fundamental performance tradeoffs in flexure mechanism design. [DOI: 10.1115/1.4023157]

Keywords: constraint-based design, spatial beam flexure, flexure mechanisms, beam constraint model, geometric nonlinearities

1 Introduction and Background

Flexure mechanisms provide guided motion via elastic deformation and are used in a variety of applications that demand high precision, minimal assembly, long operating life, and/or design simplicity [1–4]. One of the many approaches employed in the synthesis of flexure mechanisms is constraint-based design [3]. In this approach, a flexure element or module is treated as a constraint, and flexure mechanism synthesis is addressed as an exercise in creating an appropriate geometric arrangement of rigid bodies interconnected by constraints to satisfy desired mobility requirements. This geometric arrangement may be created via geometric [3–5] or analytical [6] techniques. The advantages of constraint-based design include its ability to handle spatial geometries and the physical insight that it offers into the synthesis process. However, while this approach is effective in generating conceptual designs, a more comprehensive assessment of performance and associated tradeoffs in the resulting flexure mechanisms requires greater qualitative and quantitative understanding of the constraint characteristics of the flexure elements that serve as constraints in the design.

One of the most basic flexure elements used in constraint-based design is the spatial beam flexure (Fig. 1) [6–8]. Due to its slenderness in the Y and Z directions, the stiffness values associated with bending in the XY and XZ planes and torsion about the X axis are relatively low. On the other hand, the translational stiffness along the X axis is relatively high. Given this contrast in stiffness, this beam serves as a constraint in terms of its end-displacements with respect to a reference ground—it constrains motion along the U_{XL} translation (degree of constraint (DoC)), and allows motion along the U_{YL} and U_{ZL} translations and Θ_{XL}, Θ_{YL}, and Θ_{ZL} rotations (degrees of freedom(DoF)).

While the benefits of flexure elements as constraints include their lack of friction and backlash, their reliance on elastic deformation to produce motion also results in several deviations from ideal constraint behavior [4,8]. For example, in case of the beam flexure, transverse displacements in the U_{YL}, U_{ZL}, Θ_{XL}, and Θ_{YL} DoF directions produce an error motion in the U_{XL} DoC direction. A tensile force in this DoC direction, produces stiffening in the DoF directions. Furthermore, stiffness in this DoC direction reduces with increasing displacements in the DoF directions.

These deviations of a beam flexure from ideal constraint behavior have a direct influence on the motion performance of any flexure mechanism that employs beam flexures as constraints. Figure 2 illustrates a simple 3D flexure mechanism that comprises a rigid Motion Stage connected to ground via three beam flexures. These beam flexures are geometrically arranged such that the three out-of-plane motions of the Motion Stage are constrained, while in-plane motions are allowed. Given the inherent nature of beam flexures, it may be qualitatively observed that the in-plane motions of the stage lead to undesired error motions in the out-of-plane directions due to the arc-length conservation of each beam flexure. Furthermore, the out-of-plane stiffness and load bearing capacity reduces with increasing in-plane motions. Also, the presence of large out-of-plane loads alters the in-plane stiffness and therefore range of motion.

In order to mathematically quantify these performance metrics of the flexure mechanism (motion range, load bearing capacity, stiffness, and error motions), it is essential to have a mathematical model of the constraint behavior of the constituent beam flexures. Previous analytical and experimental results have shown that geometric nonlinearities strongly influence the constraint behavior of beam flexures, especially when the DoF displacements are of the order of 10% of the beam-length [4,8–11]. These nonlinearities make the analytical modeling of the spatial beam flexure as well as the resulting flexure mechanism nontrivial. Although numerical methods such as nonlinear finite element analysis (FEA) may be used to obtain accurate results, they offer little parametric design insight.
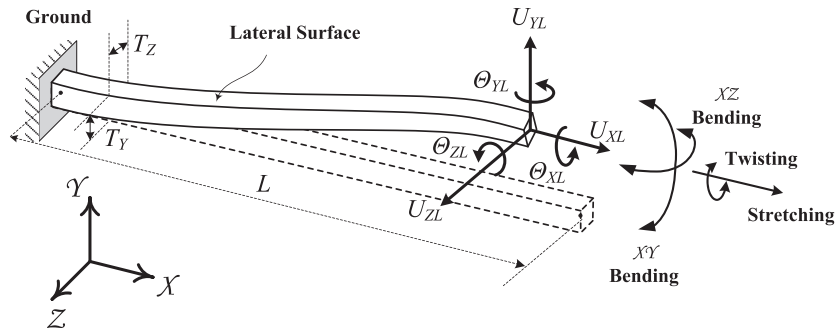
---

[1]Corresponding author.

Fig. 1 Spatial beam flexure—undeformed and deformed

To address this need, this paper presents a closed-form, parametric, analytical model that captures the relevant nonlinearities in the end load–displacement relations for a uniform and symmetric cross-section[2], slender[3], spatial beam flexure. The resulting beam constraint model, in turn, enables deterministic analysis and optimization of more complex flexure mechanisms, helps identify their performance limits and tradeoffs, and better informs constraint-based synthesis of flexure mechanisms.

The spatial beam flexure has been analyzed and studied extensively in the structural mechanics literature, as discussed in Sec. 2. This paper does not develop any new theories or formulations for beam mechanics; instead, the goal is to start with an existing beam mechanics formulation, carefully review every assumption and approximation that is made, and determine which ones to include so that relevant nonlinearities are captured (Sec. 3); and based on this, derive a new closed-form constraint model that is accurate over a practical range of loads and displacements (Secs. 4 and 5). The term "closed-form" here implies mathematical expressions that are free of infinite series, continued fractions, integrals, and limits. The accuracy of this model is validated using extensive finite elements analysis in Sec. 6. Contributions and on-going work are summarized in Sec. 7.
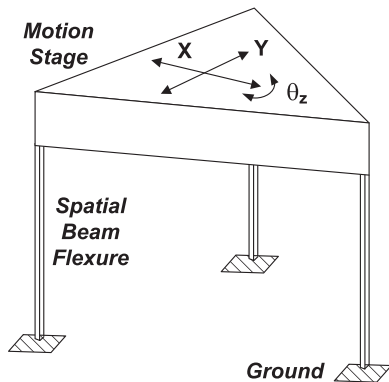

Fig. 2 A 3 DOF patial flexure mechanism

2 Background and Prior Art

Several mechanics formulations have been developed in the past to model slender, spatial beams with generalized loading. Each formulation captures certain physical components of the beam's deformation while ignoring others, depending on the desired modeling accuracy. Starting from this assumed deformation, additional approximations are made in the subsequent derivation of strain, strain energy, and governing differential equations. The extent of all these

assumptions and approximations ultimately determines what physical effects and nonlinearities are captured in a particular spatial beam model.

The well-known analytical formulation by Euler [14] assumes that "plane cross-sections remain plane and perpendicular to the neutral axis after deformation" as a slender beam bends in a plane. Shear deformation, out-of-plane warping, and in-plane distortions of the beam cross-section are neglected. With these deformation assumptions, several planar beam models have been developed with varying levels of approximations and accuracy [15]. This deformation assumption has been shown to be fairly accurate for spatial beams as well and may be used as the basis for developing strain and strain energy expressions [16]. In addition to dropping higher order terms in strain, if curvature expression is completely linearized and load-equilibrium is applied in the undeformed state, this leads to linear and completely decoupled governing differential equations that can be solved analytically. The resulting simplistic relations between end-loads and end-displacements fail to capture key nonlinear coupling effects between the bending, torsional, and axial directions [17]. These include load-stiffening in the transverse bending directions in the presence of axial loads, kinematic and elastokinematic components in the axial displacement due to transverse bending displacements, coupling between the bending directions in the presence of a torsional moment, kinematic, and elastokinematic components of the twisting angle in the presence of bending displacements, elastic coupling between axial and torsional directions, and elastokinematic coupling between the axial and torsional directions in the presence of bending displacements. As a consequence, the linear model for the spatial beam is accurate only for small bending displacements of the order of the thickness of the beam, or in the absence of torsional and axial loads.

However, if second order terms are retained in the strain expression, beam curvature is not linearized, and load-equilibrium is applied in the deformed state of the beam, one obtains nonlinear and coupled governing differential equations that capture all the above effects over large ranges of deformations and loads [16]. Solving the nonlinear governing equations for a planar beam requires the use of elliptic integrals [18] and for a spatial beam, subjected to pure bending loads, involves an infinite series of elliptic integrals [16]. Solutions based on elliptic integrals, in turn, require a numerical look-up table to obtain end-displacements for a set of given spatial end-loads. Alternatively, numerical integration can be employed to solve these nonlinear equations. Such approaches offer little design insight and are equivalent to the use of FEA in their suitability for design, evaluation, and optimization. A possible adaptation of Frisch-Fay's beam formulation is the 3D pseudo-rigid body model (PRBM) [19] that has been recently reported. This PRBM attempts to model a spatial beam as two rigid beams connected by a global torsional spring that offers torsional stiffness along three orthogonal directions. The lengths of the rigid links as well as the three stiffness values are constant and chosen to minimize the position error at the free end of the beam model with respect to a numerical solution of Frisch-Fay's beam formulation. While this PRBM is accurate in capturing the displacement of the

---

[2]Uniform implies a non-varying cross-section along the beam length. Symmetric implies equal moments of area of the beam cross-section about the Y and Z axes.
[3]Slender generally implies a length to thickness ratio greater than 20 [12,13].

beam over a large range of deformation, it is valid only for a specific loading condition and not for generalized end-loads in the six independent directions. It also does not capture fundamental elasto-kinematic effects that lead to a nonlinear stiffness variation in the axial and torsional directions with increasing transverse bending displacements. Furthermore, from the perspective of constraint-based design, it reduces a flexure element with 5 DoF to a rigid-link arrangement with only three rotational DoF.

All the formulations discussed so far neglect the deformation associated with shearing of cross-sections due to transverse forces, the in-plane distortion of cross-section, and the out-of-plane warping of cross-sections. Shearing of cross-sections due to transverse forces in short beams is captured by Timoshenko's beam theory, which also analytically shows the insignificance of this deformation component in slender beams [12]. However, out-of-plane warping has been analytically shown to exist in the presence of torsional loads [12,20]. Slender beam formulations that consider cross-sectional distortion and warping in the presence of combined bending, torsional, axial loads were developed by DaSilva [10] and Hodges and Dowell [11] for applications in helicopter rotor blade dynamics. Although these formulations were approximated to the second and third order, respectively, their mathematical complexity and nonlinearity prevented closed form load–displacement relations at the beam end.

A large body of work on beam mechanics has also been developed using the Cosserat rod theory [21], which is capable of considering the various geometric nonlinearities for bending, torsional, and axial loads. Using this theory, the helical solution of spatial beams under certain torsional and bending loads was analyzed [22]. Recent development has further generalized this theory by using nonlinear constitutive relations as well as shear and extensional effects [23–25]. However, like the Euler formulation previously, Cosserat theory does not consider in-plane distortion or out-of-plane warping of cross-sections. Moreover, given the mathematical complexity of this formulation, solutions have to be obtained via numerical techniques.

Thus, existing beam formulations and models present a tradeoff between accuracy and mathematical complexity. For the case of planar beams, there exist models that provide a compromise between these two choices. For example, the beam column theory [26] is based on the Euler's deformation assumption, retains second order terms in strain, applies load-equilibrium in the deformed configuration, but linearizes the curvature. This yields closed-form, parametric results and is valid for an intermediate range of transverse bending displacements (~10% of beam length). This formulation has been used as the basis for further approximations and generalization in the beam constraint model (BCM), which captures load-stiffening, kinematic, and elastokinematic nonlinearities in planar beams [15]. However, a similar model for end load–displacement relations of a spatial beam that

accurately captures relevant nonlinear effects but at the same time is closed-form, parametric, and generalized is not found in the existing literature, thus providing the motivation for this work. A recent attempt with a similar motivation modeled the spatial beam via two decoupled planar BCMs for the two bending planes [27]. However, this model fails to capture several critical nonlinearities such as the coupling between the two bending directions in the presence of a torsional load and the kinematic and elastokinematic components of twisting angle in the presence of bending displacements. This highlights the need for a systematic derivation that builds up from first principles and recognizes all approximations and assumptions made in arriving at a final model.

3 Nonlinear Strain Formulation

In order to determine the nonlinear strain in a slender spatial beam with any general cross-section and general end-loading, the first step is to mathematically characterize its spatial deformation. The beam deformation may be completely defined in terms of five deformation components associated with each cross-sectional plane of the beam that is perpendicular to the beam centroidal axis prior to deformation: (i) translation and rotation of this cross-section to remain plane and perpendicular to deformed centroidal axis, (ii) additional rotation of the deformed cross-sections from the previous state with respect to the centroidal axis, (iii) in-plane distortion of the cross-section, (iv) in-plane dilation/contraction of the cross-section, and (v) out-of-plane warping of the cross-section.

A sub-set of these deformations is assumed here, along the lines of previous analyses. Deformation (i) corresponds to the previously stated Euler's assumption and is central to beam bending. Deformation (ii) is associated with shear deformation in the plane of bending and was captured by Timoshenko and Goodier [12] in his exact solution of cantilever beams subjected to a transverse end force. In this analysis, the angle about the Z axis between the deformed centroidal axis and the cross-sectional plane normal was shown to be approximately $(T_Y/L)^2$ times the slope of the neutral axis, where T_Y is the thickness of the beam along Y axis. Since $(T_Y/L)^2$ is of the order of 10^{-3} or smaller for slender beams, this component of deformation is negligible and can be safely ignored. The in-plane distortion (iii) is associated with torsion of the beam. St. Venant formulated the exact solution for slender beams with any general cross-section in pure torsion and demonstrated that the in-plane distortion is exactly zero for a compatible torsional load distribution at the end surface [12,20]. For slender beams under combined end-loads, this deformation can be nonzero but is still negligible [10,11]. In the absence of any loads on the lateral surfaces of the beam, the dilation or contraction (iv) of the cross-section arises solely due to Poisson's effect in the Y and Z directions. Although this component is included in the analysis, it ultimately proves to be inconsequential, as shown later. Finally,
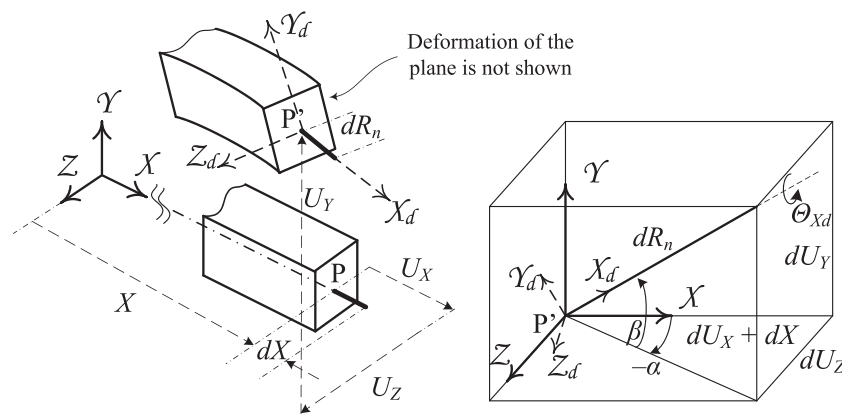

Fig. 3   Spatial kinematics of beam deformation

even though out-of-plane cross-sectional warping (**v**) has been shown to be exactly zero for a circular cross-section beam under pure torsion, it does exist in a general cross-section beam and affects the torsional constant [10–12,20], and is therefore included in this analysis.

Figure 3 illustrates a slender beam with a general cross-section that is uniform along its length subjected to general end-loading. Only the deformation component (**i**) is shown; in-plane dilation/contraction (**iv**) and out-plane warping (**v**), while included in the analysis, are not shown for simplicity of illustration.

Consider the X–Y–Z coordinate frame and a cross-section plane at distance X from the beam-root and normal to the centroidal axis of the beam before deformation, as shown in Fig. 3. Point P $(X, 0, 0)$ denotes the centroid of this cross-section plane. The first step in deformation is when this entire cross-section translates and rotates as a rigid plane. Point P translates to P′ $(X+U_X, U_Y, U_Z)$ by undergoing three mutually perpendicular translations and P′ lies on the deformed centroidal axis of the beam. A new X_d axis is defined along the tangent to this deformed centroidal axis at location P′ and is therefore normal to the deformed cross-section plane. The rotation of the cross-section as it translates from P to P′ can be captured using three Euler angles α, β, and Θ_{Xd}. The last of these angles will be referred to as the twisting angle in this paper, but it should be noted that, in general, the choice of Euler angles is not unique.

Thus, the six general displacements U_X, U_Y, U_Z, α, β, and Θ_{Xd} completely define a deformed coordinate frame X_d–Y_d–Z_d that varies with the coordinate X. Y_d and Z_d are simply the local coordinate axes of a cross-section plane in the deformed frame. Next, the out-of-plane warping is estimated to be $\lambda \cdot \kappa_{Xd}$, where λ is a warping function dependent on only the local cross-sectional coordinates Y_d and Z_d and independent of coordinate X. κ_{Xd} is the rate of twisting along the deformed centroidal axis and will be defined in terms of the derivative of the six general displacements in the following paragraphs. It should be noted that since warping would disappear if the beam was reduced to a line, λ can be set to zero along the centroidal axis without any loss of generality.

With the beam deformation thus completely defined, we next proceed to determine the Green's strain measure, ε_{ij}, [20] at any general point with coordinate position (X, Y, Z) before deformation.

$$d\vec{R}_d \bullet d\vec{R}_d - d\vec{R}_0 \bullet d\vec{R}_0$$

$$= 2\{ dX \quad dY \quad dZ \}
\begin{bmatrix}
\varepsilon_{XX} & \varepsilon_{XY} & \varepsilon_{XZ} \\
\varepsilon_{YX} & \varepsilon_{YY} & \varepsilon_{YZ} \\
\varepsilon_{ZX} & \varepsilon_{ZY} & \varepsilon_{ZZ}
\end{bmatrix}
\begin{Bmatrix} dX \\ dY \\ dZ \end{Bmatrix} \qquad (1)$$

Here $\vec{R}_0$ and $\vec{R}_d$ are the position vectors of this point before and after deformation. In the special case when the deformed point is on the neutral axis of the beam, its position vector is denoted by $\vec{R}_n$, the derivative of which is shown in Fig. 3. Using this, the final expression for nonlinear strain based on the above assumed deformation, without any further approximations, may be derived to be

$$\varepsilon_{XX} = \frac{1}{2}\left[\left(1 - Y_d\kappa_{Zd} + Z_d\kappa_{Yd} + \lambda\frac{d\kappa_{Xd}}{dR_n} \right)^2 \right.$$
$$+ \left\{ (\lambda\kappa_{Zd} - Z_d)^2 + (-\lambda\kappa_{Yd} + Y_d)^2 \right\}\kappa_{Xd}^2$$
$$\left. \times \left[\left(1 + \frac{dU_X}{dX} \right)^2 + \left(\frac{dU_Y}{dX} \right)^2 + \left(\frac{dU_Z}{dX} \right)^2 \right] - \frac{1}{2}$$
$$\varepsilon_{YY} = \frac{1}{2} - \frac{1}{2}\left(\frac{dY}{dY_d} \right)^2 + \frac{1}{2}\left(\kappa_{Xd}\frac{d\lambda}{dY_d} \right)^2 ;$$
$$\varepsilon_{ZZ} = \frac{1}{2} - \frac{1}{2}\left(\frac{dZ}{dZ_d} \right)^2 + \frac{1}{2}\left(\kappa_{Xd}\frac{d\lambda}{dZ_d} \right)^2$$
$$\gamma_{YZ} = 2\varepsilon_{YZ} = \kappa_{Xd}^2\frac{d\lambda}{dY_d}\frac{d\lambda}{dZ_d} ;$$
$$\gamma_{XY} = 2\varepsilon_{XY} = \kappa_{Xd}\frac{d\lambda}{dY_d}\left(1 - Y_d\kappa_{Zd} + Z_d\kappa_{Yd} + \lambda\frac{d\kappa_{Xd}}{dR_n} \right)$$
$$+ (\lambda\kappa_{Xd}\kappa_{Zd} - Z_d\kappa_{Xd})$$
$$\gamma_{XZ} = 2\varepsilon_{XZ} = \kappa_{Xd}\frac{d\lambda}{dZ_d}\left(1 - Y_d\kappa_{Zd} + Z_d\kappa_{Yd} + \lambda\frac{d\kappa_{Xd}}{dR_n} \right)$$
$$+ (-\lambda\kappa_{Xd}\kappa_{Yd} + Y_d\kappa_{Xd}) \qquad (2)$$

where,

$$\kappa_{Xd} = \frac{\Theta_{xd}^+\Delta_{YZ}\Delta_Y - U_Z^{++}U_Y^+\Delta_Y - U_Y^{++}U_Z^+(U_Y^+)^2}{\Delta_{YZ}\Delta_Y^2},$$

$$\kappa_{Yd} = \frac{\sin(\Theta_{xd})U_Y^{++}\Delta_{YZ} - \cos(\Theta_{xd})U_Z^{++} - \cos(\Theta_{xd})U_Y^+U_Z^+U_Y^{++} + \cos(\Theta_{xd})U_Z^{++}(U_Y^+)^2}{\Delta_{YZ}\Delta_Y^2}$$

$$\kappa_{Zd} = \frac{\cos(\Theta_{xd})U_Y^{++}\Delta_{YZ} + \sin(\Theta_{xd})U_Z^{++} + \sin(\Theta_{xd})U_Y^+U_Z^+U_Y^{++} - \sin(\Theta_{xd})U_Z^{++}(U_Y^+)^2}{\Delta_{YZ}\Delta_Y} \qquad (3)$$

where, the superscript$^+$ refers to derivative with respect to R_n, and

$$\Delta_{YZ} \overset{\Delta}{=} \sqrt{1 - \left(\frac{dU_Y}{dR_n} \right)^2 - \left(\frac{dU_Z}{dR_n} \right)^2} ; \quad \Delta_Y \overset{\Delta}{=} \sqrt{1 - \left(\frac{dU_Y}{dR_n} \right)^2}$$

$$dR_n = \sqrt{(dX + dU_X)^2 + dU_Y^2 + dU_Z^2}; \quad c(\Theta_{xd}) \overset{\Delta}{=} \cos(\Theta_{xd}); \quad s(\Theta_{xd}) \overset{\Delta}{=} \sin(\Theta_{xd})$$

Next, this nonlinear strain can be simplified without much loss of accuracy when the transverse displacements and rotations are limited to 0.1 L and 0.1, respectively. In this range, terms that are more than two orders of magnitude smaller than the primary term

in a given expression become insignificant and are dropped. This is referred to as the *second order approximation* in the rest of this paper, and leads to less than 1% cumulative approximation error in any given expression over the displacement range of interest.

Furthermore, dR_n, dY_d, and dZ_d may be equated to dX, dY, and dZ, respectively, within this second order approximation. Based on these approximations, three of the above strain components may be simplified as follows:

$$\varepsilon_{XX} \approx U'_X + \frac{1}{2}U'^2_Y + \frac{1}{2}U'^2_Z - Y\kappa_{Zd} + Z\kappa_{Yd} + \frac{1}{2}\kappa^2_{Xd}(Y^2 + Z^2) \quad (4)$$

$$\gamma_{XY} \approx \kappa_{Xd}[Y - Y_W] \quad \text{where} \quad Y_W \triangleq \frac{d\lambda}{dZ} \quad (5)$$

$$\gamma_{XZ} \approx \kappa_{Xd}[Z - Z_W] \quad \text{where} \quad Z_W \triangleq \frac{d\lambda}{dY} \quad (6)$$

κ_{Xd}, κ_{Yd}, and κ_{Zd} that are defined in expression (3) may be further simplified using the second order approximation, as follows:

$$\kappa_{Xd} \approx \Theta'_{Xd} - U''_Z U'_Y; \quad \kappa_{Yd} \approx \sin(\Theta_{Xd})U''_Y - \cos(\Theta_{Xd})U''_Z;$$
$$\kappa_{Zd} \approx \cos(\Theta_{Xd})U''_Y + \sin(\Theta_{Xd})U''_Z \quad (7)$$

It is evident that κ_{Xd} captures the rate of change of twist angle Θ'_{Xd} along the beam length, while correcting for a kinematic contribution from transverse displacements. The asymmetry between the Y and Z displacements in this expression is simply a result of the specific choice of Euler angles employed in defining the beam deformation. Since U''_Y and U''_Z are the linearized curvature of the beam in the XY and XZ planes, respectively, the latter two relations in Eq. (7) imply that, κ_{Yd} and κ_{Zd} are representative of curvatures of the beam in the X_dY_d and X_dZ_d planes, respectively, which agrees with the physical understanding of the deformed geometry. The significance of Eq. (7) is that while it partially linearizes the three curvature expressions, which is critical to reducing mathematical complexity and ultimately enabling closed-form results, it still captures the coupling between the torsional and bending directions. Full linearization of curvatures at this stage would lead to complete decoupling between the torsional and two bending directions, which is an over-simplification as discussed earlier.

The first three terms in the axial strain, given by Eq. (4), collectively represent the elastic extension in the axial direction, corrected for the kinematic effect of rotation due to bending. This captures the nonlinearity associated with beam arc-length conservation. The remaining terms depend on κ_{Xd}, κ_{Yd}, and κ_{Zd}, which arise from the combined effect of bending and torsion and depend only on X, as discussed above. Although the last of these three terms is significantly smaller than the others, it is retained because it is the only remaining term in the absence of bending and axial loads. Under this condition, it captures the trapeze effect of elastic coupling between the axial and torsional directions. It is noteworthy that the contribution of cross-sectional warping in the ε_{XX} strain is negligible in the displacement range of interest, therefore does not appear in the simplified ε_{XX} expression (4). The shear strains given in Eqs. (5) and (6) depend on the torsion rate κ_{Xd} and warping function λ.

The simplified nonlinear strain expressions given by Eqs. (4)–(6) are in agreement with Hodges and Dowell [11] and DaSilva [10]. Strain components ε_{YY} and ε_{ZZ} are associated with in-plane contraction and arise due to Poisson's effect in the absence of any direct Y and Z direction forces on the beam's lateral surfaces. While non-negligible, they prove to be inconsequential as seen in the next section and are therefore not simplified further. The strain component γ_{YZ} is associated with in-plane distortion and can be shown to be four orders of magnitude smaller than γ_{XY} and γ_{XZ}. This component can therefore be neglected, which is consistent with the original assumption of ignoring the in-plane distortion.

Thus, a careful choice of deformation components, use of Green's strain measure, partial linearization of curvatures, and the second order approximation in the strain components, all help capture the relevant physical effects and nonlinearities in a slender beam over an intermediate displacement range, while limiting the mathematical complexity of the strain formulation.

4 Nonlinear Strain Energy and Beam Governing Differential Equations

As the first step in deriving the beam governing equation using energy methods, the strain energy for the spatial beam flexure is expressed below by assuming linear material properties.

$$V = \frac{E}{2}\int_{\text{vol}} \varepsilon^2_{xx} dAdX + \frac{G}{2}\int_{\text{vol}} \left(\gamma^2_{xy} + \gamma^2_{xz}\right) dAdX \quad (8)$$

Here E and G are the elastic modulus and shear modulus, respectively, while A is the cross-sectional area. Due to the slenderness of the beam, the variation of stresses σ_{YY} and σ_{ZZ} is close to zero. However, since there are no externally applied stresses on the lateral surfaces of the beam, σ_{YY} and σ_{ZZ} remain zero throughout the beam. Therefore, the ε_{YY} and ε_{ZZ} strain components do not contribute to the strain energy.

There are two components of the strain energy: the first integral above is the strain energy due to axial strain that arises from transverse bending and axial extension, and the second term represents the energy due to the shear strains that arise due to torsion. This strain energy expression may be expanded using the strain expressions from Eqs. (4)–(6).

$$V = \frac{E}{2}\int_{\text{vol}} \left(U'_X + \frac{1}{2}U'^2_Y + \frac{1}{2}U'^2_Z\right)^2 dAdX$$
$$+ \frac{E}{2}\int_{\text{vol}} 2\left(U'_X + \frac{1}{2}U'^2_Y + \frac{1}{2}U'^2_Z\right)(-Y\kappa_{Zd} + Z\kappa_{Yd})dAdX$$
$$+ \frac{E}{2}\int_{\text{vol}} \{\kappa^2_{Xd}(Y^2 + Z^2)\}(-Y\kappa_{Zd} + Z\kappa_{Yd})dAdX$$
$$+ \frac{E}{2}\int_{v} (-Y\kappa_{Zd} + Z\kappa_{Yd})^2 dAdX$$
$$+ \frac{E}{2}\int_{\text{vol}} \left(U'_X + \frac{1}{2}U'^2_Y + \frac{1}{2}U'^2_Z\right)[\kappa^2_{Xd}(Y^2 + Z^2)]dAdX$$
$$+ \frac{E}{8}\int_{\text{vol}} \{\kappa^2_{Xd}(Y^2 + Z^2)\}^2 dAdX$$
$$+ \frac{G}{2}\int_{\text{vol}} \kappa^2_{Xd}\{(Y - Y_W)^2 + (Z - Z_W)^2\}dAdX$$
$$\triangleq I_1 + I_2 + I_3 + I_4 + I_5 + I_6 + I_7 \quad (9)$$

The seven individual integrals in V are denoted by I_1–I_7, in the order that they are listed. Of these, the integrals I_2 and I_3 are identically zero by the definition of the centroidal axis. For a slender beam with twisting angle Θ_{Xd} limited to ± 0.1, it may be shown that integral I_6 is at least four orders of magnitude smaller than integral I_1, and is therefore dropped. Next, the strain energy expression is simplified by recognizing that the beam curvatures, given in Eq. (7), are only dependent on the axial coordinate X. Thus, each volume integral can be decomposed into a double integral over the cross-section and a single integral over X.

$$V = \frac{EA}{2}\int_0^L (\bar{U}'_X)^2 dX + \frac{EI}{2}\int_0^L (U''^2_Y + U''^2_Z)dX$$
$$+ EI\int_0^L (\bar{U}'_X)\kappa^2_{Xd}dX + \frac{GJ}{2}\int_0^L \kappa^2_{Xd}dX$$
$$\text{where} \quad \bar{U}'_X \triangleq \left(U'_X + \frac{1}{2}U'^2_Y + \frac{1}{2}U'^2_Z\right) \quad (10)$$

The first integral I_1 above describes energy associated with axial extension. Through U'_Y and U'_Z, it also captures the geometric coupling between the bending and axial directions. The second

term, I_4, captures the strain energy associated with bending. The third term, I_5, captures the coupling between the torsion and axial extension directions. Finally, the last term I_7 captures the energy solely from torsion. In the last step of deriving Eq. (10), a symmetric beam cross-section is assumed, which implies that the two principal bending moments of area (I_{YY} and I_{ZZ}) are identical and equal to I. Due to this symmetry, the polar moment of area is equal to $2I$. The torsion constant J is, in general, different from the polar moment of area due to warping [12,13], as shown below.

$$\int_A Y^2 dA = \int_A Z^2 dA \overset{\triangle}{=} I; \quad \int_A YZ dA = 0$$
$$\int_A (Y^2 + Z^2) dA = 2I; \quad \int_A \left\{ (Y - Y_W)^2 + (Z - Z_W)^2 \right\} dA \overset{\triangle}{=} J$$

$$(11)$$

Once the total strain energy for the spatial beam has been obtained, the principle of virtual work (PVW) [20] may be applied to generate the beam differential equations and boundary conditions. According to the PVW, the virtual work done by external forces over a set of geometrically compatible but otherwise arbitrary "virtual" displacements is equal to the change in the strain energy due to these "virtual" displacements

$$\delta W = \delta V \qquad (12)$$

$U_X, U_Y, U_Z, \Theta_{Xd}, U'_Y,$ and U'_Z may be chosen as the six generalized coordinates which, along with their boundary conditions, completely define the deformation and strain energy of the beam. The variation of the beam strain energy expression (10) with respect to these generalized coordinates is given by

$$\delta V = \delta I_1 + \delta I_4 + \delta I_5 + \delta I_7 \qquad (13)$$

where

$$\delta I_1 = EA\left\{ \bar{U}'_X \left(\delta U_X + U'_Y \delta U_Y + U'_Z \delta U_Z \right) \right\} \Big|_0^L - EA \int_0^L \bar{U}''_X \delta U_X dX$$
$$- EA \int_0^L \left(\bar{U}'_X U'_Y \right)' \delta U_Y dX - EA \int_0^L \left(\bar{U}'_X U'_Z \right)' \delta U_Z dX$$

$$\delta I_4 = EI \left(U''_Y \delta U'_Y + U''_Z \delta U'_Z - U'''_Y \delta U_Y - U'''_Z \delta U_Z \right) \Big|_0^L$$
$$+ EI \int_0^L \left(U_Y^{iv} \delta U_Y + U_Z^{iv} \delta U_Z \right) dX$$

$$\delta I_5 = EI \left\{ \kappa_{Xd}^2 \left(\delta U_X + U'_Y \delta U_Y + U'_Z \delta U_Z \right) \right\} \Big|_0^L - EI \int_0^L \left(\kappa_{Xd}^2 \right)' \delta U_X dX$$
$$- EI \int_0^L \left(\kappa_{Xd}^2 U'_Y \right)' \delta U_Y dX - EI \int_0^L \left(\kappa_{Xd}^2 U'_Z \right)' \delta U_Z dX$$
$$+ 2EI \left[\bar{U}'_X \kappa_{Xd} \delta \Theta_{Xd} - \bar{U}'_X \kappa_{Xd} \left(U'_Y \delta U'_Z + U''_Z \delta U_Y \right) \right.$$
$$\left. + \left(\bar{U}'_X \kappa_{Xd} U'_Y \right)' \delta U_Z \right] \Big|_0^L - 2EI \left[\int_0^L \left\{ \left(\bar{U}'_X \kappa_{Xd} U'_Y \right)'' \delta U_Z \right. \right.$$
$$\left. \left. - \left(\bar{U}'_X \kappa_{Xd} U''_Z \right)' \delta U_Y \right\} dX \right] - 2EI \int_0^L \left\{ \kappa_{Xd} \bar{U}'_X \right\}' \delta \Theta_{Xd} dX$$

$$\delta I_7 = GJ \left[\left\{ \kappa_{Xd} \delta \Theta_{Xd} - \kappa_{Xd} \left(U'_Y \delta U'_Z + U''_Z \delta U_Y \right) + \left(\kappa_{Xd} U'_Y \right)' \delta U_Z \right\} \right] \Big|_0^L$$
$$- GJ \left[\int_0^L \left\{ \left(\kappa_{Xd} U'_Y \right)'' \delta U_Z - \left(\kappa_{Xd} U''_Z \right)' \delta U_Y \right\} dX \right]$$
$$- GJ \int_0^L \kappa'_{Xd} \delta \Theta_{Xd} dX$$

This variation of the strain energy is expressed in terms of the six generalized virtual displacements $\delta U_X, \delta U_Y, \delta U_Z, \delta \Theta_{Xd}, \delta U'_Y,$ and $\delta U'_Z$ (all of which are variables in the X coordinate), and their

boundary values at the fixed end, which are all identically equal to zero, and the free end, which are defined to be $\delta U_{XL}, \delta U_{YL}, \delta U_{ZL}, \delta \Theta_{XdL},$ and $\delta U'_{YL},$ and $\delta U'_{ZL}$.

Next, the virtual work done by external loads $\boldsymbol{F_{XL}}, \boldsymbol{F_{YL}}, \boldsymbol{F_{ZL}}, \boldsymbol{M_{XL}}, \boldsymbol{M_{YL}},$ and $\boldsymbol{M_{ZL}}$ may be conveniently expressed as

$$\delta W = \boldsymbol{F_{XL}} \delta U_{XL} + \boldsymbol{F_{YL}} \delta U_{YL} + \boldsymbol{F_{ZL}} \delta U_{ZL} + \boldsymbol{M_{XL}} \delta \Theta_{XL}$$
$$+ \boldsymbol{M_{YL}} \delta \Theta_{YL} + \boldsymbol{M_{ZL}} \delta \Theta_{ZL} \qquad (14)$$

where $\delta U_{XL}, \delta U_{YL}, \delta U_{ZL}, \delta \Theta_{XL}, \delta \Theta_{YL},$ and $\delta \Theta_{ZL}$ represent a slightly different set of six independent virtual displacements at the beam end in the respective directions of the six external loads.

Applying PVW, the variation of strain energy is equated to virtual work. Next, to derive the load–displacement relations, the six virtual end-displacements in Eq. (14) have to be expressed in terms of the previous set of six virtual end-displacements that are used in the variation of the strain energy in Eq. (13). This would allow coefficients of the same virtual end-displacements on both sides of Eq. (12) to be equated. Specifically, this requires expressing virtual rotations $\delta \Theta_{XL}, \delta \Theta_{YL},$ and $\delta \Theta_{ZL}$ as functions of $\delta U_{XL}, \delta U_{YL}, \delta U_{ZL}, \delta \Theta_{XdL}, \delta U'_{YL},$ and $\delta U'_{ZL}$. Since virtual rotations can be chosen to be arbitrarily small, they can be represented as vectors. Therefore, the virtual rotations at the beam end may be expressed as variations of the corresponding Euler angles (Fig. 2)

$$\delta \Theta_{XL} \hat{i} + \delta \Theta_{YL} \hat{j} + \delta \Theta_{ZL} \hat{k}$$
$$= -\delta \alpha \hat{j} \big|_L + \left\{ \cos(\alpha) \hat{k} - \sin(\alpha) \hat{i} \right\} \delta \beta \big|_L$$
$$+ \left\{ \frac{1 + U'_X}{1 + \bar{U}'_X} \hat{i} + \frac{U'_Y}{1 + \bar{U}'_X} \hat{j} + \frac{U'_Z}{1 + \bar{U}'_X} \hat{k} \right\} \delta \Theta_{Xd} \Big|_L \qquad (15)$$

where $\delta \alpha = -\dfrac{\delta U'_Z}{1 + U'_X} + \dfrac{U'_Z \delta U'_X}{(1 + U'_X)^2}$ and

$$\delta \beta = \frac{\delta U'_Y}{1 + U'_X + \frac{1}{2} U'^2_Z} - \frac{U'_Y \left(\delta U'_X + U'_Z \delta U'_Z \right)}{\left(1 + U'_X + \frac{1}{2} U'^2_Z \right)^2}$$

For the range of end displacements considered, $\bar{U}'_{XL}, U'_{XL}, U'_{YL},$ and U'_{ZL} are of the order of $10^{-3}, 10^{-2}, 10^{-1},$ and 10^{-1}, respectively. Therefore, second order approximations are made to simplify Eq. (15) to yield

$$\delta \Theta_{XL} \approx \delta \Theta_{XdL} - U'_{ZL} \delta U'_{YL} + U'_{ZL} U'_{YL} \left(\delta U'_{XL} + U'_{ZL} \delta U'_{ZL} \right)$$
$$\delta \Theta_{YL} \approx -\delta U'_{ZL} + U'_{ZL} \delta U'_{XL} + U'_{YL} \delta \Theta_{XdL}$$
$$\delta \Theta_{ZL} \approx \delta U'_{YL} - U'_{YL} \left(\delta U'_{XL} + U'_{ZL} \delta U'_{ZL} \right) + U'_{ZL} \delta \Theta_{XdL} \qquad (16)$$

Using Eq. (16), the left hand side of PVW in Eq. (12) can be expressed in terms of $\delta U_{XL}, \delta U_{YL}, \delta U_{ZL}, \delta \Theta_{XdL}, \delta U'_{YL},$ and $\delta U'_{ZL}$. The only remaining dependent displacement variable now is $\delta U'_{XL}$. Although its dependence on the other virtual displacements is not known at this stage, we know that it is mathematically independent of δU_{XL}. Therefore, the coefficients of δU_{XL} and δU_X on both sides of Eq. (12) can be respectively compared and equated.

$$\left(EA \bar{U}'_X + EI \kappa_{Xd}^2 \right) \big|_L = \boldsymbol{F_{XL}}, \quad \text{and} \quad \left(EA \bar{U}'_X + EI \kappa_{Xd}^2 \right)' = 0$$

These two relations imply that

$$EA \bar{U}'_X + EI \kappa_{Xd}^2 = \text{constant} = \boldsymbol{F_{XL}} \qquad (17)$$

This relation may now be used to derive the geometric dependence of U'_{XL} on the other displacement variables. Since $\partial \sigma_{YY}/\partial Y$ and $\partial \sigma_{YZ}/\partial Z$ are approximately zero due to the absence of lateral forces and in-plane distortion, respectively, $\partial \tau_{XY}/\partial X$ turns out to

be zero from the elemental equilibrium condition in the Y direction

$$\frac{\partial \tau_{YX}}{\partial X} + \frac{\partial \sigma_{YY}}{\partial Y} + \frac{\partial \sigma_{YZ}}{\partial Z} = 0 \Rightarrow \frac{\partial \tau_{YX}}{\partial X} = 0 \qquad (18)$$

This result, along with Eq. (5), implies that κ_{Xd} remains constant with X. This, along with Eq. (17), implies that $\bar{U}'_X$ remains constant with X. This knowledge, along with the definition of $\bar{U}'_X$ in Eq. (10), yields the following relation:

$$\delta U'_X = -U'_Y \delta U'_Y - U'_Z \delta U'_Z \qquad (19)$$

The value of $\delta U'_{XL}$ is now substituted back in Eq. (16), which reduces to

$$\delta \Theta_{XL} = \delta \Theta_{XdL} - U'_{ZL} \delta U'_{YL}$$
$$\delta \Theta_{YL} = -\delta U'_{ZL} - U'_{YL} U'_{ZL} \delta U'_{YL} + U'_{YL} \delta \Theta_{XdL}$$
$$\delta \Theta_{ZL} = \delta U'_{YL} + U'_{ZL} \delta \Theta_{XdL} \qquad (20)$$

This allows one to express all the terms on the right and left hand sides of Eq. (12) using the same set of six virtual end-displacements. Now, the respective coefficients of all the virtual displacements on both sides of this equation are compared and equated.

Comparing the coefficients of $\delta \Theta_{XdL}$ and $\delta \Theta_{Xd}$, we get

$$\left\{ GJ \left(1 + \frac{2EI}{GJ} \bar{U}'_X \right) \kappa_{Xd} \right\} \bigg|_L = M_{XdL} \quad \text{and}$$
$$\left\{ \left(1 + \frac{2EI}{GJ} \bar{U}'_X \right) \kappa_{Xd} \right\}' = 0$$

where $M_{XdL} \overset{\Delta}{=} M_{XL} + U'_{YL} M_{YL} + U'_{ZL} M_{ZL}$

$$\Rightarrow \kappa_{Xd} = \left\{ \Theta'_{Xd} - U''_Z U'_Y \right\} = \text{constant} = \frac{M_{XdL}}{GJ} \left(1 + \frac{2EI}{GJ} \bar{U}'_X \right)^{-1} \qquad (21)$$

Moment M_{XdL} is simply the equivalent torsional moment expressed along the deformed centroidal axis at the free end of the beam. Equations (17) and (21) can now be solved simultaneously for $\bar{U}'_X$ and Θ_{Xd}. Since these two quantities are of the order of 10^{-2} and 10^{-1}, respectively, second order approximations are made in arriving at the following two simplified relations.

$$U'_{XL} + \frac{1}{2} U'^2_{YL} + \frac{1}{2} U'^2_{ZL} \approx \frac{F_{XL}}{EA} - \frac{I}{A} \cdot \frac{M^2_{XdL}}{G^2 J^2} \qquad (22)$$

$$\Theta'_{Xd} - U''_Z U'_Y \approx \frac{M_{XdL}}{GJ} - \frac{2I M_{XdL} F_{XL}}{G^2 J^2 A} \qquad (23)$$

The above two equations are the governing differential equations associated with extension and torsion, respectively. Equation (22) clearly captures beam arc-length conservation, which leads geometric coupling between the axial and two bending directions. Additionally, it also captures the weak coupling between axial and torsional directions, also known as the trapeze effect [28]. This coupling is also evident in the torsion Eq. (23), which additionally captures the geometric dependence of twisting angle on the two bending displacements.

Equating the coefficients of the remaining virtual displacements, δU_{YL}, δU_Y, δU_{ZL}, δU_Z, $\delta U'_{YL}$, and $\delta U'_{ZL}$, two more governing differential equations associated with bending in the XY and XZ planes are obtained, along with four natural boundary conditions at the beam end.

$$EI U^{iv}_Y - F_{XL} U''_Y + M_{XdL} U'''_Z = 0;$$
$$EI U^{iv}_Z - F_{XL} U''_Z - M_{XdL} U'''_Y = 0 \qquad (24)$$

$$F_{YL} = F_{XL} U'_{YL} - EI U'''_{YL} - M_{XdL} U''_{ZL}$$
$$F_{ZL} = F_{XL} U'_{ZL} - EI U'''_{ZL} + M_{XdL} U''_{YL}$$
$$M_{YL} = -EI U''_{ZL} + M_{XdL} U'_{YL}$$
$$\left(1 + U'^2_{ZL} \right) M_{ZL} = EI U''_{YL} + M_{XdL} U'_{ZL} \Rightarrow M_{ZL} \approx EI U''_{YL}$$
$$+ M_{XdL} U'_{ZL} \qquad (25)$$

Equation (24) captures the stiffening effect of axial force on the bending displacements and the coupling between the two bending directions due to the axial moment. The final approximation in the natural boundary condition, although not necessary, is made to maintain consistency with previous second order approximations. The beam governing differential Eqs. (22)–(24) derived here are in agreement with previously derived nonlinear beam models [10,11] that contain more terms and are therefore mathematically more complex. When subjected to the same assumptions and second order approximations that have been made here, these previous models reduce to the results presented here. However, we have taken a more basic approach of deriving the governing equations from first principles, recognizing every assumption and approximation made in the process, and highlighting the physical implications of these mathematical steps to avoid accidental elimination of relevant nonlinear effects.

Although capturing the various nonlinear coupling effects renders the governing equations of extension and torsion to be nonlinear, the bending equations are still linear and coupled in U_Y and U_Z. This allows Eq. (24), along with associated boundary conditions (25), to be solved using linear algebra [29] and then the results can be substituted in Eqs. (22) and (23) to solve for U_X and θ_{Xd}, which provide the two geometric constraint conditions. The results may also be substituted in the strain energy term. This procedure is employed in Sec. 5 to obtain closed-form load–displacement relations, geometric constraint conditions, and strain energy expression for the slender, symmetric, spatial beam in terms of it end-displacements and end-loads.

5 End Load–Displacement Relations for Symmetric Spatial Beam

At this point in the analysis, all the loads and displacements are normalized per the following scheme to make the equations and results compact

$$m_{z1} \overset{\Delta}{=} \frac{M_{ZL} L}{EI}, \quad m_{y1} \overset{\Delta}{=} \frac{M_{YL} L}{EI}, \quad m_{xd1} \overset{\Delta}{=} \frac{M_{XdL} L}{EI},$$
$$f_{z1} \overset{\Delta}{=} \frac{F_{ZL} L^2}{EI}, \quad f_{y1} \overset{\Delta}{=} \frac{F_{YL} L^2}{EI}, \quad f_{x1} \overset{\Delta}{=} \frac{F_{XL} L^2}{EI},$$
$$v \overset{\Delta}{=} \frac{VL}{EI}, \quad u_y \overset{\Delta}{=} \frac{U_Y}{L}, \quad u_z \overset{\Delta}{=} \frac{U_Z}{L}, \quad u_{y1} \overset{\Delta}{=} \frac{U_{YL}}{L},$$
$$u_{z1} \overset{\Delta}{=} \frac{U_{ZL}}{L}, \quad x \overset{\Delta}{=} \frac{X}{L}, \quad \theta_{xd} \overset{\Delta}{=} \Theta_{Xd}, \quad \theta_{xd1} \overset{\Delta}{=} \Theta_{XdL}$$

Based on this, the beam governing differential Eqs. (22)–(24), can be normalized as follows:

$$u^{iv}_y - f_{x1} u''_y + m_{xd1} u'''_z = 0; \quad u^{iv}_z - f_{x1} u''_z - m_{xd1} u'''_y = 0 \qquad (26)$$

$$u'_{x1} + \frac{1}{2} u'^2_{y1} + \frac{1}{2} u'^2_{z1} \approx \frac{f_{x1}}{k_{33}} - \frac{2 m^2_{xd1}}{k_{33} k^2_{44}} \qquad (27)$$

$$\left\{\theta'_{xd} - u''_z u'_y\right\} \approx \frac{m_{xd1}}{k_{44}} - \frac{2m_{xd1}f_{x1}}{k_{33}k_{44}^2} \tag{28}$$

where,

$$k_{33} \triangleq \frac{12L^2}{T_Y^2}, \quad k_{44} \triangleq \frac{GJ}{EI}, \quad m_{xd1} \triangleq m_{x1} + u'_{y1}m_{y1} + u'_{z1}m_{z1}$$

The solution of Eq. (26) leads to relations between the end-loads and end-displacements by employing the following normalized geometric and natural boundary conditions obtained from Eq. (25)

$$f_{y1} = f_{x1}u'_{y1} - u'''_{y1} - m_{xd1}u''_{z1}; \quad f_{z1} = f_{x1}u'_{z1} - u'''_{z1} + m_{xd1}u''_{y1}$$

$$m_{y1} = -u''_{z1} + m_{xd1}u'_{y1}; \quad m_{z1} = u''_{y1} + m_{xd1}u'_{z1}$$

$$u_y(0) = 0; \quad u_z(0) = 0; \quad u'_y(0) = 0; \quad u'_z(0) = 0$$

$$u_{y1} \triangleq u_y(1); \quad u_{z1} \triangleq u_z(1); \quad u'_{y1} \triangleq u'_y(1); \quad u'_{z1} \triangleq u'_z(1) \tag{29}$$

The end load–displacement relations are of the following form, where each element in the 4×4 stiffness matrix is a transcendental function of the end loads f_{x1} and m_{xd1}.

$$\left\{f_{y1} \quad m_{z1} \quad f_{z1} \quad m_{y1}\right\}^T = [K(f_{x1}, m_{xd1})]\left\{u_{y1} \quad u'_{y1} \quad u_{z1} \quad -u'_{z1}\right\}^T \tag{30}$$

To express this result in a form that is mathematically concise and provides insight into the geometric effects and nonlinearities that are relevant to constraint characterization, we carry out a Taylor series expansion of each stiffness element in terms of the axial and torsional loads, f_{x1} and m_{xd1} and drop third and higher power terms.

$$\left\{f_{y1} \quad m_{z1} \quad f_{z1} \quad m_{y1}\right\}^T = [H_1]\left\{u_{y1} \quad u'_{y1} \quad u_{z1} \quad -u'_{z1}\right\}^T$$
$$- [2f_{x1}H_2 + m_{xd1}(2H_3 + H_7)]$$
$$\times \left\{u_{y1} \quad u'_{y1} \quad u_{z1} \quad -u'_{z1}\right\}^T$$
$$- [f_{x1}^2 H_4 + m_{xd1}f_{x1}H_5 + m_{xd1}^2 H_6]$$
$$\times \left\{u_{y1} \quad u'_{y1} \quad u_{z1} \quad -u'_{z1}\right\}^T + \cdots \tag{31}$$

where

$$H_1 \triangleq \begin{bmatrix} 12 & -6 & 0 & 0 \\ -6 & 4 & 0 & 0 \\ 0 & 0 & 12 & 6 \\ 0 & 0 & 6 & 4 \end{bmatrix}, \quad H_2 \triangleq \begin{bmatrix} -\frac{3}{5} & \frac{1}{20} & 0 & 0 \\ \frac{1}{20} & -\frac{1}{15} & 0 & 0 \\ 0 & 0 & -\frac{3}{5} & -\frac{1}{20} \\ 0 & 0 & -\frac{1}{20} & -\frac{1}{15} \end{bmatrix},$$

$$H_3 \triangleq \frac{1}{4}\begin{bmatrix} 0 & 0 & 0 & -2 \\ 0 & 0 & -2 & -1 \\ 0 & -2 & 0 & 0 \\ -2 & -1 & 0 & 0 \end{bmatrix}$$

$$H_4 \triangleq \begin{bmatrix} \frac{1}{700} & -\frac{1}{1400} & 0 & 0 \\ -\frac{1}{1400} & \frac{11}{6300} & 0 & 0 \\ 0 & 0 & \frac{1}{700} & \frac{1}{1400} \\ 0 & 0 & \frac{1}{1400} & \frac{11}{6300} \end{bmatrix},$$

$$H_5 \triangleq \frac{1}{60}\begin{bmatrix} 0 & 0 & 0 & 1 \\ 0 & 0 & 1 & 0 \\ 0 & 1 & 0 & 0 \\ 1 & 0 & 0 & 0 \end{bmatrix}, \quad H_6 \triangleq \frac{1}{20}\begin{bmatrix} 4 & -2 & 0 & 0 \\ -2 & 1 & 0 & 0 \\ 0 & 0 & 4 & 2 \\ 0 & 0 & 2 & 1 \end{bmatrix}$$

$$H_7 \triangleq \begin{bmatrix} 0 & 0 & 0 & 0 \\ 0 & 0 & 0 & 1 \\ 0 & 0 & 0 & 0 \\ 0 & 0 & 0 & 0 \end{bmatrix}$$

Next, the $u_y(x)$ and $u_z(x)$ solutions to the bending Eq. (26) are substituted into Eqs. (27) and (28), which upon integration provide the solution for the axial extension and twisting, respectively. Once again, these solutions contain 4×4 matrices, each nonzero element of which is a transcendental function of the end loads f_{x1} and m_{xd1}. A Taylor series expansion of each element, followed by truncation of higher order terms produces the following two constraint relations, expressed in terms of the end displacements and loads of the beam.

$$u_{x1} = \frac{f_{x1}}{k_{33}} - \frac{m_{xd1}^2}{k_{44}^2 k_{33}} + \left\{u_{y1} \quad u'_{y1} \quad u_{z1} \quad -u'_{z1}\right\}[H_2]$$
$$\times \left\{u_{y1} \quad u'_{y1} \quad u_{z1} \quad -u'_{z1}\right\}^T + \left\{u_{y1} \quad u'_{y1} \quad u_{z1} \quad -u'_{z1}\right\}$$
$$\times \left[f_{x1}H_4 + \frac{1}{2}m_{xd1}H_5\right]\left\{u_{y1} \quad u'_{y1} \quad u_{z1} \quad -u'_{z1}\right\}^T + \cdots \tag{32}$$

$$\theta_{xd1} = \frac{m_{xd1}}{k_{44}} - \frac{2m_{xd1}f_{x1}}{k_{33}k_{44}^2} + \left\{u_{y1} \quad u'_{y1} \quad u_{z1} \quad -u'_{z1}\right\}[H_3]$$
$$\times \left\{u_{y1} \quad u'_{y1} \quad u_{z1} \quad -u'_{z1}\right\}^T + \left\{u_{y1} \quad u'_{y1} \quad u_{z1} \quad -u'_{z1}\right\}$$
$$\times \left[m_{xd1}H_6 + \frac{1}{2}f_{x1}H_5\right]\left\{u_{y1} \quad u'_{y1} \quad u_{z1} \quad -u'_{z1}\right\}^T + \cdots \tag{33}$$

The series truncations produce less than 1% loss of accuracy in each respective relation over an f_{x1} range of ± 5 and an m_{xd1} range of ± 0.1, while providing considerable mathematical simplicity and physical insight. The former represents a typical DoC direction bearing force, while the latter represents the normalized moment associated with a rotation of 0.1 along the θ_x DoF. The $[H_1]$ matrix in relation (31) represents the linear elastic stiffness associated with the four transverse bending displacements. The $[H_2]$ matrix captures load stiffening in these directions in the presence of axial load f_{x1} (Eq. (31)) and a corresponding purely kinematic contribution of bending displacements to the axial displacement (Eq. (32)). The $[H_3]$ and $[H_7]$ matrices captures load stiffening in the bending directions in the presence of torsional moment m_{xd1} (Eq. (31)) and reveals a coupling between the two bending planes in the presence of this moment. Corresponding to this, the $[H_3]$ matrix also captures the purely kinematic contribution of bending displacements to the twisting angle (Eq. (33)). Although the $[H_4]$, $[H_5]$, and $[H_6]$ matrices make a negligible contribution in Eq. (31), they capture the important elastokinematic effects in Eqs. (32) and (33). In the axial direction, $[H_4]$ provides

an additional compliance with respect to axial load f_{x1} and $[H_5]$ provides an additional compliance with respect to axial moment m_{xd1}, in the presence of transverse bending displacements. Similarly, in the twisting direction, $[H_5]$ provides an additional compliance with respect to axial load f_{x1} and $[H_6]$ provides an additional compliance with respect to axial moment m_{xd1}, in the presence of transverse bending displacements. These relations also highlight the unique status of the twisting rotation θ_{dx1}. Based on physical intuition, this twisting direction appears to be a DoF, like the transverse displacements $u_{y1}, u_{y1}', u_{z1},$ and u_{z1}', because of its low stiffness. However, mathematically, it behaves more like the u_{x1} DoC and is dictated by the constraint relation (33), which is analogous to constraint relation (32). The $[H_1]$–$[H_7]$ matrices are dimensionless and valid for any beam size and shape, as long as the beam is uniform, symmetric, and slender. Therefore, elements of these matrices are subsequently referred to as the *beam characteristic coefficients*.

Next, the strain energy expression (10) may be further simplified using Eqs. (27) and (28), and can be stated as follows after normalization

$$v = \frac{1}{2}\int_0^1 \left(u_y''^2 + u_z''^2 \right) dx + \frac{m_{xd1}^2}{2k_{44}} + \frac{f_{x1}^2}{2k_{33}} - \frac{2m_{xd1}^2 f_{x1}}{k_{33}k_{44}^2} \quad (34)$$

The $u_y(x)$ and $u_z(x)$ solutions to the bending Eq. (26) obtained previously can be substituted above to produce the total strain energy in terms of end-displacements $u_{y1}, u_{y1}', u_{z1},$ and u_{z1}' and loads m_{xd1} and f_{x1} as follows:

$$
\begin{aligned}
v = \frac{1}{2} & \left\{ u_{y1} \quad u_{y1}' \quad u_{z1} \quad -u_{z1}' \right\} \\
& \times \left[H_1 + \frac{f_{x1}^2}{2}H_4 + \frac{m_{xd1}f_{x1}}{2}H_5 + \frac{m_{xd1}^2}{2}H_6 \right] \\
& \times \left\{ u_{y1} \quad u_{y1}' \quad u_{z1} \quad -u_{z1}' \right\}^T + \frac{m_{xd1}^2}{2k_{44}} + \frac{f_{x1}^2}{2k_{33}} - \frac{2m_{xd1}^2 f_{x1}}{k_{33}k_{44}^2}
\end{aligned}
$$
$$(35)$$

This strain energy expression allows a designer to treat the spatial beam as a single lumped entity, with all the relevant nonlinearities captured, when analyzing a flexure mechanism consisting of multiple spatial beam flexures using energy methods. Overall, the transverse load–displacement relations (31), the geometric constraint relations in axial extension (32) and torsion (33), and the strain energy expression (35), collectively represent a closed-form, parametric, nonlinear model that captures constraint characteristics of a slender, symmetric, spatial beam; this model is subsequently referred to as the spatial-beam constraint model (spatial-BCM).

6   Validation

The results of the previous section are validated via nonlinear FEA using ANSYS™. For these simulations, the beam dimensions were taken to be $L = 0.1$ m and $T_Y = T_Z = 0.0025$ m, and Young's modulus and Poisson's ratio were assumed to be 210 GPa and 0.3, respectively. For each beam, 400 BEAM188 elements were used, with the *restrained warping*, *torsional shear*, and *large deformation* options turned on. To verify individual elements of $[H_1]$, three of the four displacements among $u_{y1}, u_{y1}', u_{z1},$ and u_{z1}' are set to zero, while the fourth displacement is varied from -0.1 to 0.1. When axial and torsional loads f_{x1} and m_{xd1} are set to zero, the reaction loads $f_{y1}, m_{z1}, f_{z1},$ and m_{y1} provide the elements of $[H_1]$. In Fig. 4, each nonzero (i, j) element of $[H_1]$ is plotted with respect to the respective transverse displacement that was varied, while keeping others zero, for its determination.

The $[H_2]$ matrix is obtained by measuring the u_{x1} displacement for different values of $u_{y1}, u_{y1}', u_{z1},$ and u_{z1}' while setting m_{xd1} and f_{x1} to zero, as per Eq. (32). Similarly, the $[H_3]$ matrix is

obtained by measuring the θ_{xd1} rotation for different values of $u_{y1}, u_{y1}', u_{z1},$ and u_{z1}' while setting m_{xd1} and f_{x1} to zero, as per Eq. (33). Finally, as per Eq. (31), the $[H_7]$ matrix is verified by setting m_{xd1} and u_{z1}' to nonzero values and $u_{y1}, u_{y1}', u_{z1},$ and f_{x1} to zero, and measuring m_{z1}. It should be noted that this will also capture the effect of $[H_1]$, which is separated out to obtain $[H_7]$. Nonzero elements of the $[H_2]$, $[H_3]$, and $[H_7]$ matrices are plotted in Fig. 5. These results show that the elastic bending stiffness captured by the $[H_1]$ matrix, and load-stiffening and kinematic effects captured by the $[H_2]$, $[H_3]$, and $[H_7]$ in the BCM are accurate to within 1% with respect to FEA.

Matrices $[H_4]$ and $[H_5]$ capture the nonlinear elastokinematic effects in the X direction and are obtained by measuring the u_{x1} for different values of $u_{y1}, u_{y1}', u_{z1},$ and u_{z1}' while setting $m_{xd1} = 0$ or $f_{x1} = 0$, one at a time. This calculation requires subtraction of the kinematic displacement component associated with $[H_2]$, which has already been validated above. The nonzero elements of $[H_4]$ are plotted in Fig. 6. Because the u_{x1} displacement is dominated by the kinematic effect given by $[H_2]$, the estimate of $[H_4]$ through FEA is affected relatively more by the numerical errors in FEA, which cause the discrepancy seen in Fig. 6. Nevertheless, the maximum discrepancy between FEA and BCM results for the $[H_4]$ matrix, which contributes an elastokinematic component to u_{x1}, is still within 6%.

Next, the nonzero elements of $[H_5]$ are plotted in Fig. 7. This represents a weaker elastokinematic contribution to u_{x1} compared
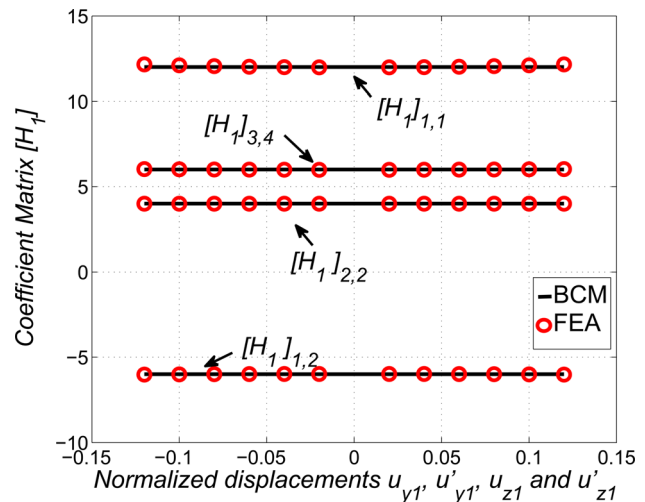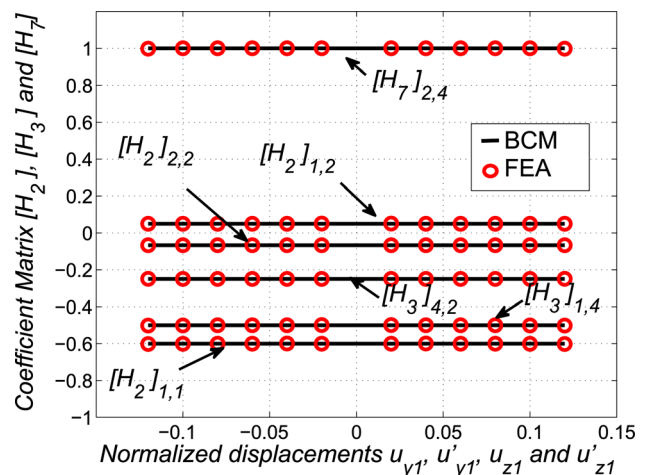

Fig. 4   Elastic matrix [H_1]

Fig. 5   Kinematic matrices [H_2], [H_3], and [H_7]
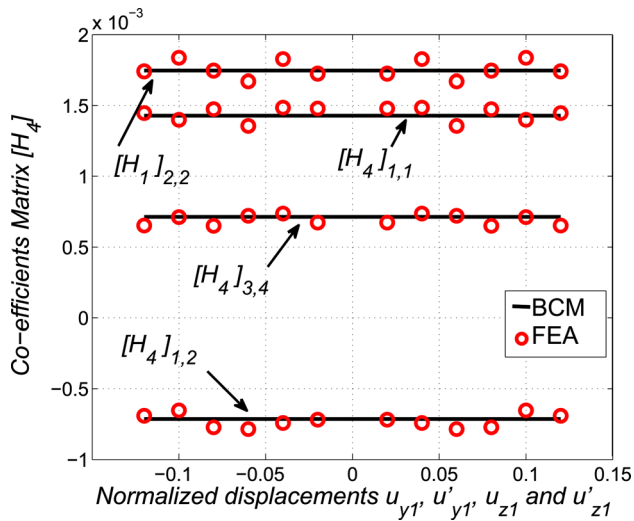
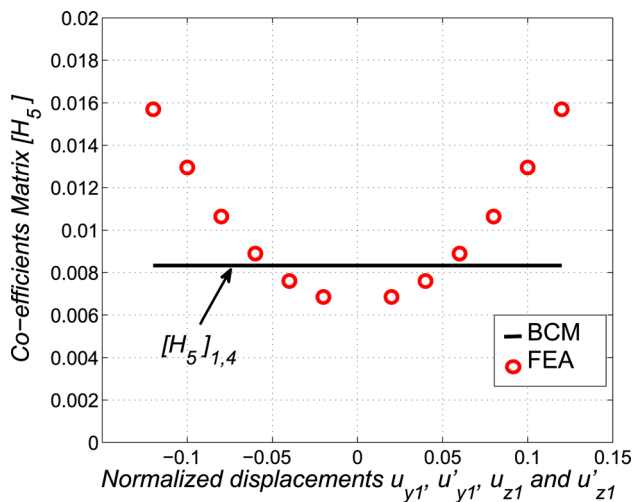**Fig. 6 Elastokinematic matrix [H_4]**

Fig.7 Elastokinematic matrix [H_5]

to [H_4], and therefore the discrepancy between FEA and BCM is much greater. Even though the orders of magnitude are comparable, the trends no longer agree. At this point, the second order assumptions made in the BCM derivation start to become weak, leading to the observed discrepancy.

The elastokinematic effects captured by the [H_5] and [H_6] matrices in Eq. (33) contribute additional compliance in the θ_x direction in the presence of transverse bending displacements. However, these effects are even smaller than those along the X direction, over the load and displacement range of interest. As a result, the [H_6] matrix is difficult to estimate and validate via FEA. In physical terms, these effects do not play a significant role in the constraint characteristics of the spatial beam. Since θ_x is a DoF direction, it nominally exhibits a high linear compliance (1/k_{44}); the small additional compliance due to these elastokinematic effects does not make much difference.

Separately, the model was also verified to be accurate when all six loads are applied simultaneously. For a particular case, with $F_{XL} = 300$N; $F_{YL} = 40$N; $F_{ZL} = 80$N; $M_{XL} = 0.1$Nm; $M_{YL} = 4$Nm; $M_{ZL} = -0.5$Nm; chosen such that the resulting displacements are within the relevant range, the discrepancy between FEA and BCM in predicting the bending displacements u_{y1}, u'_{y1}, u_{z1}, and u'_{z1} was to found to be less than 2.1% while the error in predicting u_{x1} and θ_{x1} was 1.8% and 3.4%, respectively.

7 Conclusion

While several spatial beam models exist, they are either too trivial to capture the nonlinear effects that influence the constraint characteristics of spatial beams, or mathematically too complex to serve the goals of constraint-based flexure design, analysis, and optimization. In this paper, we employ an existing beam mechanics formulation for a slender, spatial beam, but identify the simplifications possible when the two principal moments of area are equal ($I_{YY} = I_{ZZ}$). Starting from first principles, we carefully make specific assumptions and approximations that are valid for an intermediate range of bending displacements and twisting angle (normalized values of ± 0.1), and for normalized axial loads within ± 10. This not only allows reduction of the mathematical complexity to a manageable level but also captures all the relevant nonlinear effects in a compact, closed-form, parametric manner. The final model is based on the Euler's deformation assumption along with small out-of-plane cross-sectional warping, Green's strain measure, second order approximation of strain terms, partial linearization of curvature expressions, and truncation of higher power terms in axial and torsional loads.

This results in a new spatial-beam constraint model that comprises load–displacement relations in bending directions, geometric constraint relations in axial and torsional directions, and a strain energy expression – all in terms of the six end-loads and six end-displacements. These relations capture all the geometric nonlinearities that affect the constraint characteristics of the beam: load-stiffening in the bending directions in the presence of an axial load, coupling between the bending directions in the presence of a torsional moment, kinematic and elastokinematic components in the axial displacement and twisting angle due to transverse bending displacements, and the trapeze effect coupling between axial and torsional directions. These are all validated to be accurate within a few percent using nonlinear FEA over the above-mentioned displacement and load range of interest, which is justified by typical material failure limits in flexure mechanisms. The model also reveals an interesting mathematical similarity between the twisting angle and axial displacement, even though the former is generally recognized as a DoF and the latter as DoC.

Since no assumption, other than symmetry (i.e., $I_{YY} = I_{ZZ}$), is made for the beam cross-section, this model is applicable to beams with circular, square, and other regular polygon shaped cross-sections. When the symmetry of the cross-section is broken (i.e., $I_{YY} \neq I_{ZZ}$), the above simplification and resulting closed-form model is no longer possible. However, certain observations can be made based on the beam mechanics. It can be shown that the twist would not only be kinematically dependent on the bending displacements but also elastically dependent on the bending loads. This implies the existence of nonzero twists for zero torsional moment, which in turn means that the bending directions would be coupled even in the absence of a torsional moment. This would make the beam governing equations in the bending direction nonlinear and very difficult to solve in a closed-form manner. However, the primary nonlinear effects (load-stiffening, kinematic, and elastokinematic) arising due to the axial force f_{x1} and beam arc-length conservation are largely independent of the twist and therefore would remain the same.

We envision that the qualitative and quantitative understanding of the constraint characteristics of the spatial beam gained via this model will facilitate deterministic analysis and optimization of more complex flexure mechanisms that employ spatial beams, help identify their performance limits and tradeoffs, and better inform constraint-based synthesis of flexure mechanisms. To facilitate this goal, we are currently developing a nonlinear strain energy formulation that is consistent with the spatial beam model presented here. This strain energy formulation, when employed with energy methods, will lead to mathematically efficient derivation of analytical load–displacement results for flexure mechanisms comprising multiple spatial beam flexures.

Acknowledgment

References

[1] Jones, R. V., 1988, *Instruments and Experiences: Papers on Measurement and Instrument Design*, Wiley, New York.

[2] Smith, S. T., 2000, *Flexures: Elements of Elastic Mechanisms, Gordon and Breach Science Publishers*, New York.

[3] Blanding, D. K., 1999, *Exact Constraint: Machine Design Using Kinematic Principles, ASME Press*, New York.

[4] Awtar, S., 2004, "Analysis and Synthesis of Planer Kinematic XY Mechanisms," Sc. D., Massachusetts Institute of Technology, Cambridge, MA.

[5] Hopkins, J. B., and Culpepper, M. L., 2010, "Synthesis of Multi-Degree of Freedom, Parallel Flexure System Concepts Via Freedom and Constraint Topology (FACT)—Part I: Principles," Precis. Eng., **34**, pp. 259–270.

[6] Su, H. J., and Tari, H., 2010, "Realizing Orthogonal Motions With Wire Flexures Connected in Parallel," ASME J. Mech. Des., **132**, p. 121002.

[7] Sen, S., and Awtar, S., 2010, "Nonlinear Constraint Model for Symmetric Three-Dimensional Beams," Proceedings of IDETC/CIE 2010, Montreal, Canada, pp. 607–618.

[8] Awtar, S., Slocum, A. H., and Sevincer, E., 2006, "Characteristics of Beam-based Flexure Modules," J. Mech. Des., **129**, pp. 625–639.

[9] Zelenika, S., and DeBona, F., 2002, "Analytical and Experimental Characterization of High Precision Flexural Pivots Subjected to Lateral Loads," Precis. Eng., **26**, pp. 381–388.

[10] DaSilva, M. R. M. C., 1988, "Non-Linear Flexural-Flexural-Torsional-Extensional Dynamics of Beams—I. Formulation," Int. J. Solids Struct., **24**, pp. 1225–1234.

[11] Hodges, D. H., and Dowell, E. H., 1974, "Nonlinear Equations of Motion for the Elastic Bending and Torsion of Twisted Non-Uniform Rotor Blades," NASA Technical Note D-7818.

[12] Timoshenko, S., and Goodier, J. N., 1969, *Theory of Elastisity*, McGraw-Hill, New York.

[13] Crandall, S. H., Dahl, N. C., and Lardner, T. J., 1972, *An Introduction to the Mechanics of Solids*, McGraw-Hill Book Company, New York.

[14] Euler, L., 1744, Methodus Inveniendi Lineas Curvas Maximi Minimive Proprietate Gaudentes, "Lausannæ, Genevæ, apud Marcum-Michaelem Bousquet & socios". Available at http://archive.org/details/methodusinvenie00eulegoog

[15] Awtar, S., and Sen, S., 2010, "A Generalized Constraint Model for Two-Dimensional Beam Flexures: Non-Linear Load-Displacement Formulation," ASME J. Mech. Des., **132**, p. 0810091.

[16] Frisch-Fay, R., 1962, *Flexible Bars*, Butterworth & Co. Ltd., London.

[17] Przemieniecki, J. S., 1968, *Theory of Matrix Structural Analysis*, McGraw-Hill, New York.

[18] Bisshop, K. E., and Drucker, D. C., 1945, "Large Deflections of Cantilever Beams," Q. Appl. Math., **3**(3), pp. 272–275.

[19] Ramirez, I. A., and Lusk, C., 2011, "Spatial-Beam Large-Deflection Equations and Pseudo-Rigid Body Model for Axisymmetric Cantilever Beams," Proceedings of the IDETC/CIE 2011, Washington D. C., pp. 43–49.

[20] Shames, I. H., and Dym, C. L., 1985, *Energy and Finite Element Methods in Structural Mechanics*, Taylor and Francis, New York, NY.

[21] Rubin, M. B., 2000, *Cosserat Theories: Shells, Rods, and Points*, Springer, New York.

[22] Kirchhoff, G., 1859, "Uber des Gleichgewicht und die Bewegung eines unendlich dunner elasticschen Slabes," J. Reine Agnew. Math., **56**, pp. 285–313.

[23] Chouaie, B. N., and Maddocks, J. H., 2004, "Kirchhoff's Problem of Helical Equilibria of Uniform Rods," J. Elasticity, **77**, pp. 221–247.

[24] Whitman, A. B. and DeSilva, C. N., 1974, "An Exact Solution in a Nonlinear Theory of Rods," J. Elasticity, **4**(4), pp. 265–280.

[25] Antman, S. S., 1974, "Kirchhoff's Problem for Nonlinearly Elastic Rods," Q. Appl. Math., **32**(3), pp. 221–240.

[26] Krylov, A. N., 1931, Calculation of Beams on Elastic Foundation, Russian Academy of Sciences, St. Petersburg.

[27] Hao, G., Kong, X., and Reuben, R. L., 2011, "A Nonlinear Analysis of Spatial Compliant Parallel Modules: Multi-Beam Modules," Mech. Mach. Theory, **46**, pp. 680–706.

[28] Popescu, B., and Hodges, D. H., 1999, "Asymptotic Treatment of the Trapeze Effect in Finite Element Cross-Sectional Analysis of Composite Beams," Int. J. Non-Linear Mech., **34**, pp. 709–721.

[29] Sen, S., and Awtar, S., 2011, "Nonlinear Strain Energy Formulation to Capture the Constraint Characteristics of a Spatial Symmetric Beam," Proceedings of the IDETC/CIE 2011, Washington, pp. 127–135.